THE STATISTICAL DISTRIBUTIONS FOR THE ELEVATION, VELOCITY AND ACCELERATION OF THE SURFACE OF WIND WAVES

Honda, Tadao
Research Institute for Applied Mechanics, Kyushu University : Research Associate

Mitsuyasu, Hisashi
Research Institute for Applied Mechanics, Kyushu University : Professor

https://doi.org/10.5109/6610200

出版情報：Reports of Research Institute for Applied Mechanics. 24 (76), pp.31-48, 1976-07. 九州大学応用力学研究所
バージョン：
権利関係：

Reports of Research Institute for Applied Mechanics
Vol. XXIV, No. 76, 1976

THE STATISTICAL DISTRIBUTIONS FOR THE ELEVATION, VELOCITY AND ACCELERATION OF THE SURFACE OF WIND WAVES*

By Tadao HONDA** and Hisashi MITSUYASU***

Water surface elevations $\eta(t)$, vertical surface velocities $\dot{\eta}(t)$ and vertical surface accelerations $\ddot{\eta}(t)$ of wind-generated waves have been measured in a laboratory wind wave channel by using resistance-type wave gauges combined with an electronic differentiation circuits. Probability distributions of the values of $\eta(t)$, $\dot{\eta}(t)$ and $\ddot{\eta}(t)$ have been determined from the records.

In an initial stage of wave generation, i.e., when wind waves are generated at short fetches and low wind speeds, the observed distributions for $\eta(t)$, $\dot{\eta}(t)$ and $\ddot{\eta}(t)$ show good fit to the distributions given by successive sum of a Gram-Charlier series, which has been derived following the formulation of LONGUET-HIGGINS (1963), by taking the weakly nonlinear effect into account.

However, when wind waves develop with increasing wind speeds and fetches, the observed distributions deviate gradually from the Gram-Charlier series. Particularly, the deviations are remarkable for the distribution of $\ddot{\eta}(t)$.

When the wind speed increases, the observed distributions of $\eta(t)$, $\dot{\eta}(t)$ and $\ddot{\eta}(t)$ show the following characteristics: (i) the skewnesses of the distributions of $\eta(t)$ and $\dot{\eta}(t)$ decrease slightly, (ii) the skewness of $\ddot{\eta}(t)$ changes, at some wind speed, from positive small values to relatively large negative values, (iii) the kurtosis of the distribution of $\eta(t)$ decreases slightly but that of $\dot{\eta}(t)$ increases slightly and these characteristics seem to depend not so much on fetches, (iv) the kurtosis of the distribution of $\ddot{\eta}(t)$ increases rapidly.

1. Introduction

To a first approximation, random sea surface may be regarded as a linear superposition of statistically independent free waves and can be described by its two-dimensional power spectrum. Furthermore, it is a natural consequence

* This paper was originally presented in the Journal of the Oceanographical Society of Japan, Vol. 31, No. 2. Some data are added at this time.

** Research Associate, Research Institute for Applied Mechanics, Kyushu University.
*** Professor, Research Institute for Applied Mechanics, Kyushu University.

of a random walk theory and the Central Limit Theorem that the probability distribution of such random surface is Gaussian. In fact, the Gaussian assumption for sea waves has been approximately supported by many observations in the sea (for example, RUDNICK [1], PIERSON [2], LONGUET-HIGGINS *et al.*, [3]). However, closer observations of the wind waves in the sea and in a laboratory tank have shown that this assumption is not necessarily satisfied when the nonlinear effects are not negligible (KINSMAN[4], MITSUYASU [5]).

Recently, the statistical probability density function for a variable that is "weakly nonlinear" has been derived theoretically by LONGUET-HIGGINS [5]. He has mathematically shown that the probability density for random surface elevations of sea waves can be given by a Gram-Charlier series; not in the form generally used as an empirical fit for observed distributions, but in a modified form due to Edgeworth.

The main purposes of the present study are firstly to measure as accurately as possible the probability density function for surface elevations $\eta(t)$, vertical surface velocities $\dot{\eta}(t)$ and vertical surface accelerations $\ddot{\eta}(t)$ of wind waves which are generated in a laboratory tank, and secondly to compare these measured distributions with the theoretical distributions derived respectively from the ordinary linear theory and from the nonlinear theory given by LONGUET-HIGGINS [6]. To the authors knowledge, there are quite few data on the statistical properties of $\dot{\eta}(t)$ and $\ddot{\eta}(t)$. Since the high frequency components play an important role in the distributions for $\dot{\eta}(t)$ and $\ddot{\eta}(t)$, particular attentions have been paid for measuring wind waves up to very high frequencies (approximately 50 Hz).

The experimental equipments and techniques for measuring $\eta(t)$, $\dot{\eta}(t)$ and $\ddot{\eta}(t)$ are briefly described in 2. In 3 we outline the linear theory and weakly nonlinear theory of the statistical distribution of a random sea surface. These theories are then applied, in 4, to the distributions of surface elevation $\eta(t)$, vertical velocity $\dot{\eta}(t)$ and acceleration $\ddot{\eta}(t)$ of wind wave in a laboratory tank. Some discussions on the measured results are stated in 5.

2. Experimental data

The experiments were carried out in a long narrow wind wave channel illustrated in Figure 1. The glass-enclosed test section of the channel is 80 cm high, 60 cm wide and 850 cm long. The water depth was set to be 38 cm and wind speeds U_r which were mesured by a Pitot-static tube at the entrance of the test section, were varied over the range from 5 to 15 m/sec in 2.5 m/sec step. Waves were measured, along the centerline of the test section, at the following fetches; $F = 105$, 225, 345, 585, and 825 cm. The surface elevations of wind waves $\eta(t)$ were measured by two different kinds of resistance-type wave gauges. Three of these gauges were single platimum wires 0.1 mm in diameter located at fetches of 105, 225 and 345 cm

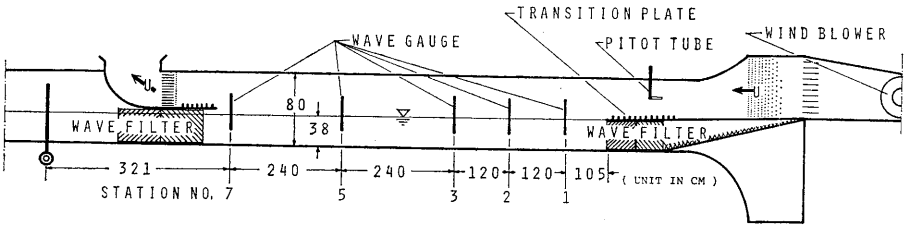

Fig. 1. Wind wave channel.

respectively. The other two gauges were parallel platinum wires, 0.1 mm in diameter and separated by 1 mm, which were set at fetches of 585 cm and 825 cm.

The frequency responses of these wave gauges were tested carefully. The amplitude response factor was approximately unity up to 40 Hz for the parallel-wire wave gauge and up to 80 Hz for the single-wire wave gauge. Therefore, it can be said that the wind-wave records measured in the present study cover the very wide frequency ranges up to capillary wave range.

At fetches, 105, 225, and 345 cm, the surface vertical velocities $\dot{\eta}(t)$ were measured by sending the output signal from the single wire wave gauge to an electronic differentiation circuit, after passing through a low-pass filter (cut-off frequency = 56 Hz) in order to remove higher frequency electric noise. Similarly, the surface vertical accelerations $\ddot{\eta}(t)$ were measured at the same fetches by sending the signals from first differentiation circuit to second differentiation circuit (cut-off frequency = 56 Hz). The differentiations by these electronic circuits were almost complete in the frequency range below the cut-off frequency.

All these signals of $\eta(t)$, $\dot{\eta}(t)$ and $\ddot{\eta}(t)$ were recorded simultaneously on a magnetic tape of 14-channel data recorder. The wave data recorded on the magnetic tape were reproduced and digitized by using a high speed A-to-D converter and the statistical analysis of the data was done on a FACOM 270 -20 computer.

The experimental conditions and the conditions relating to the statistical data analysis are summarized as follows: water depth $d = 38$ cm

Ur: 5, 7.5, 10, 12.5, 15 m/sec

F cm	105	225	345	585	825
Recorded signals	$\eta, \dot{\eta}, \ddot{\eta}$	$\eta, \dot{\eta}, \ddot{\eta}$	$\eta, \dot{\eta}, \ddot{\eta}$	η	η

sampling frequency of the data: 200 Hz
number of digitized data: 20480 (102.4 sec)

More detailed descriptions of the equipments and techniques may be referred to the previous paper (MITSUYASU and HONDA [7),8)]).

3. The outline of the theory

Let $p(\eta)$ be the probability density that a variable such as the surface elevation in random sea, η, falls to the interval between η and $\eta+d\eta$. Taking the Fourier transform of $p(\eta)$, one has

$$\phi(it) = \int_{-\infty}^{\infty} p(\eta) e^{it\eta} d\eta$$

$$= 1 + \frac{\mu_1}{1!}(it) + \frac{\mu_2}{2!}(it)^2 + \cdots, \tag{1}$$

where $\mu_n (n = 1, 2, 3, \cdots)$ is the n-th. moment of the distribution. If we define $\mathbf{K}(it)$ as

$$\mathbf{K}(it) = \log_e \phi(it) = \frac{\kappa_1}{1!}(it) + \frac{\kappa_2}{2!}(it)^2 + \cdots, \tag{2}$$

we have

$$\kappa_1 = \mu_1, \quad \kappa_2 = \mu_2 - \mu_1^2, \quad \kappa_3 = \mu_3 - 3\mu_1\mu_2 + 2\mu_1^3 \quad ,$$

$$\kappa_4 = \mu_4 - 4\mu_1\mu_3 - 3\mu_2^2 + 12\mu_1^2\mu_2 - 6\mu_1^4 \quad ,$$

$$\kappa_5 = \mu_5 - 5\mu_1\mu_4 - 10\mu_2\mu_3 + 20\mu_1^2\mu_3 + 30\mu_1\mu_2^2 - 60\mu_1^3\mu_2 + 24\mu_1^5 \quad .$$

By taking the inverse Fourier transform of $\phi(it)$ and substituting $t = s/\kappa_2^{1/2}$, $\eta - \kappa = f\kappa_2^{1/2}$, we have

$$p(\eta) = \frac{1}{2\pi\kappa_2^{1/2}} \int_{-\infty}^{\infty} \exp\left[-\frac{1}{2}(s^2 + 2ifs)\right] \cdot \exp\left[\sum_{n=3}^{\infty} \frac{\lambda_n}{n!}(is)^n\right] ds \quad , \tag{3}$$

where

$$\lambda_n = \kappa_n / \kappa_2^{n/2}, \quad (n = 3, 4, \cdots).$$

The second exponential term can be expanded, giving

$$\exp\left[\sum_{n=3}^{\infty} \frac{\lambda_n}{n!}(is)^n\right] = 1 + \frac{\lambda_3}{6}(is)^3 + \frac{\lambda_4}{24}(is)^4 + \frac{\lambda_5}{120}(is)^5$$

$$+ \left(\frac{\lambda_6}{720} + \frac{\lambda_3^2}{72}\right)(is)^6 + \cdots, \tag{4}$$

and we have identically

$$\frac{1}{(2\pi)^{1/2}} \int_{-\infty}^{\infty} \exp\left[-\frac{1}{2}(s^2 + 2ifs)\right](is)^n ds = e^{-f^2/2} H_n(f) \quad , \tag{5}$$

where H_n denotes the Hermite polynomial of degree n. Substituting (4), (5),

into (3), we have finally the probability density function in the form

$$p(\eta) = \frac{e^{-f^2/2}}{(2\pi\kappa_2)^{1/2}}\left\{1+\frac{\lambda_3}{6}H_3+\frac{\lambda_4}{24}H_4+\frac{\lambda_5}{120}H_5+\left(\frac{\lambda_6}{720}+\frac{\lambda_3^2}{72}\right)H_6+\cdots\right\}. \qquad (6)$$

3-1. Linear theory

The linear spectral representation of the sea surface elevation at a fixed place and time can be expressed as the sum of more than a finite number of simple sine waves;

$$\eta^{(N)} = \sum_{i=1}^{N} a_i\eta_i = \sum_{i=1}^{N} a_i\cos(\mathbf{k}_i\cdot\mathbf{x}-\sigma_i t+\theta_i) \quad , \qquad (7)$$

where a_i and θ_i are amplitude and phase constants, chosen randomly so that $a_i \cos\theta_i$ and $a_i \sin\theta_i$ are jointly normal, with θ_i uniformly distributed, position vector $\mathbf{x}$ and time t are fixed, and $\mathbf{k}_i$ is vector wave number. Later, we shall make $N\to\infty$. The amplitude a_i are such that in any small but fixed region $d\mathbf{k}$, $\sum_n \overline{a_i}^2/2 = \mathbf{E}(\mathbf{k})d\mathbf{k}$, say. Here $\mathbf{E}(\mathbf{k})$ is the directional wave spectrum.

Let $p_1(y)$ be such a probability density that $\eta^{(1)}$ falls on the interval between y and $y+dy$. By taking Fourier transform of $p_1(\eta)$, we have

$$\phi(it) = \int_{-\infty}^{\infty} p_1(\eta)e^{ity}dy \quad .$$

Now we consider the probability density $p_N(\eta)$ which is defined as the probability density that the sea surface elevation $\eta^{(N)}$ composed from N independent wave components falls on the interval between η and $\eta+d\eta$. The probability density $p_N(\eta)$ can be obtained as follows; the sea surface elevation $\eta^{(N)}$ can be consider as

$$\eta^{(N)} = \eta^{(1)} + \eta^{(N-1)} \quad .$$

The probability density $p_N(\eta)$ is such the probability density that, when the first term $\eta^{(1)}$ takes the value λ, say, the second term $\eta^{(N-1)}$ takes the value $\eta-\lambda$. Since $\eta^{(1)}$ and $\eta^{(N-1)}$ are statistically independent, the joint probability density is given by $p_1(\lambda)\ p_{N-1}(\eta-\lambda)$, so that $p_N(\eta)$ can be obtained by integrating $p_1(\lambda)\ p_{N-1}(\lambda-\eta)$ with respects to λ from $-\infty$ to ∞;

$$p_N(\eta) = \int_{-\infty}^{\infty} p_1(\lambda)p_{N-1}(\eta-\lambda)d\lambda \quad .$$

From the convolution theorem, $\phi_N(it)$, the inverse transform of $p_N(\eta)$, is given by

$$\phi_N(it) = \phi_1(it)\phi_{N-1}(it) = [\phi_1(it)]^N \quad . \qquad (8)$$

Comparing now Equations (2) and (8), $p_N(\eta)$ can be expressed in the form,

by substituting $\lambda_n/N^{n/2-1}$ for λ_n in (4),

$$p_N(\eta) = \frac{e^{-f^2/2}}{(2\pi\kappa_2)^{1/2}}\left\{1+\frac{\lambda_3}{6N^{1/2}}H_3+\frac{\lambda_4}{24N}H_4+\cdots\right\} \quad .$$

If we consider the limiting case $N\to\infty$, we have

$$\lim_{N\to\infty} p_N(\eta) = e^{-f^2/2}(2\pi\kappa_2)^{1/2} \quad . \tag{9}$$

Equation (9) shows that the probability distribution of the sea surface elevation expressed as the sum of more than a finite number of linear random wave components is given by the Gaussian distribution.

3-2. Nonlinear theory

The nonlinear spectral representation of the sea surface elevations η can be expressed mathematically in the form,

$$\eta = \sum_i \alpha_i\eta_i + \sum_i\sum_j \alpha_{ij}\eta_i\eta_j + \sum_i\sum_j\sum_k \alpha_{ijk}\eta_i\eta_j\eta_k + \cdots \quad , \tag{10}$$

where α_i, α_{ij}, α_{ijk} etc., are constants and η_i, η_j, η_k etc., are independent random variables symmetrically distributed about 0 with variance V_i, V_j, V_k and so on (LONGUET-HIGGINS [6]). With each values of i is associated a vector wave number $\mathbf{k}_i$. We define each V_i in such a way that over any small but fixed region $d\mathbf{k}$

$$\sum_{\mathbf{k}\ni d\mathbf{k}} V_i = \mathbf{E}(\mathbf{k})d\mathbf{k}$$

We can obtain each term in (10) by solving the nonlinear wave equations using perterbation method (see LONGUET-HIGGINS [6]). The first term in (10) corresponds to the first order solution and the second term to the second order solution and so on.

If let $p(\eta)$ be the probability density for η and $\phi(it)$ its Fourier transform, from (1), (2), (4), (5) we have (6) as the expression for the probability density $p(\eta)$. Since λ_n is order $V^{n/2-1}$ (LONGUET-HIGGINS [6]), we rearrange (6) in the ascending powers of $V^{1/2}$, so that we have finally

$$p(\eta) = \frac{e^{-f^2/2}}{(2\pi\kappa_2)^{1/2}}\left\{1+\frac{\lambda_3}{6}H_3+\frac{\lambda_4}{24}H_4+\frac{\lambda_3^2}{72}H_6+\frac{\lambda_5}{120}H_5+\cdots\right\} \quad . \tag{11}$$

Equation (11) shows that the probability distribution for the surface elevation of weakly nonlinear random waves is given by successive sum of a Gram-Charlier series. Comparing (9) with (11), it can be seen that the successive terms that follow the second in (11) express the effects of nonlinearities.

4. Comparison of the theory with experiment

The probability distribution $p(\eta)$ of random sea surface $\eta(x, t)$ can be, to a linear approximation, given by Equation (9). This equation is the well known Gaussian distribution. Taking the weakly nonlinear effect into account, the probability distribution $p(\eta)$ for random sea surface can be represented by Equation (11).

The distribution (11) corresponds quite closly to Edgeworth's form of the type A Gram-Charlier series. Equation (11) differs from the theoretical distribution used by LONGUET-HIGGINS [6] by the term

$$\frac{e^{-f^2/2}}{\sqrt{2\pi\kappa_2}} \cdot \frac{\lambda_5}{120} H_5 \quad . \tag{12}$$

As will be shown later, this term improves the agreements between the theory and experiment for the case of the surface elevation η, but not for the cases of $\dot{\eta}$ and $\ddot{\eta}$.

The Gaussian distribution (9) and the Gram-Charlier series (11) are compared with observed distributions of the laboratory wind waves which were measured very accurately up to high frequency (approximately up to 50 Hz).

In a first step, higher order terms, $\lambda^2{}_3$ and λ_5, are neglected in Equation (10), leaving only λ_3 and λ_4, so that $p(\eta)$ is given by

$$p(\eta) = \frac{e^{-f^2/2}}{\sqrt{2\pi\kappa_2}}\left(1+\frac{\lambda_3}{6}H_3+\frac{\lambda_4}{24}H_4\right) \quad . \tag{13}$$

This form will be denoted by Gram-Charlier (I). In the next step, only λ_5 is neglected. Thus,

$$p(\eta) = \frac{e^{-f^2/2}}{\sqrt{2\pi\kappa_2}}\left(1+\frac{\lambda_3}{6}H_3+\frac{\lambda_4}{24}H_4+\frac{\lambda^2{}_3}{72}H_6\right) \quad , \tag{14}$$

which will be denoted by Gram-Charlier (II). The probability distribution with full terms explicitly given in (11) will be denoted by Gram-Charlier (III).

The Gaussian, Gram-Charlier (I), (II) and (III) are compared in Figure 2 with the probability density histogram for an example of the distribution of the surface elevation $\eta(t)$ measured at fetch $F = 825$ cm for wind speed $U_r = 15$ m/sec. In Figure 2 x-axises are normalized by σ_η that denotes the standard deviation of the distribution of $\eta(t)$. It can be seen from Figure 2 that the observed distribution fits quite well to the Gram-Charlier (III) as compare to the other theoretical distributions, and that the departure of the observed distribution from the Gaussian distribution is very large. This fact suggests that the higher order approximation of the Gram-Charlier series can fit the distributions of the surface elevation of wind waves with appreciable nonlinearity, though the sum of χ^2 are not so small as will be shown

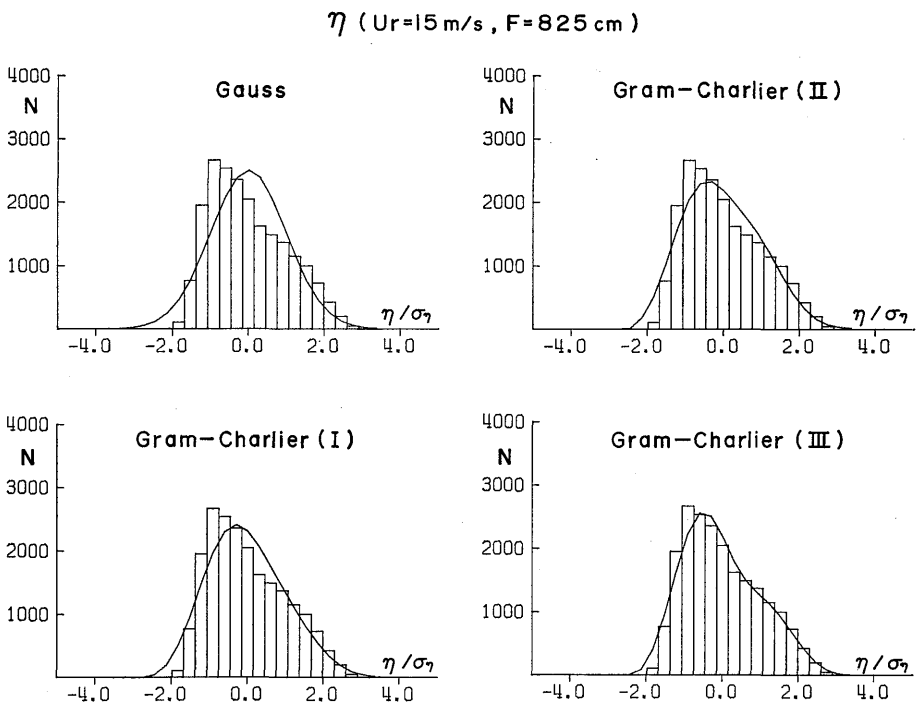

Fig. 2. The comparisons of the measured distributions for the surface elevation $\eta(t)$ with various theoretical distributions, Gaussian, Gram-Charlier (I), (II) and (III). Wave data ($F = 825$ cm, $U_r = 15$ m/sec).

later.

Similarly, in Figure 3 is shown the comparison of theoretical probability distributions with the histogram for a surface vertical acceleration $\ddot{\eta}(t)$ measured at $F = 345$ cm for $U_r = 15$m/sec. In Figure 3, x-axises are normalized by $\sigma_{\ddot{\eta}}$ that denotes the standard deviation of the distribution of $\ddot{\eta}(t)$. It can be seen from Figure 3 that in a strict sense none of the theoretical distributions fits to the observed distribution for $\ddot{\eta}(t)$. The sum of χ^2 for the Gaussian, the Gram-Charlier (I), (II) and (III) are shown in the following table.

	η	$\ddot{\eta}$
Gauss	1782	3443
Gram-Charlier (I)	607	858
Gram-Charlier (II)	450	899
Gram-Charlier (III)	195	2261
Experimental conditions	$U_r = 15$ m/sec, $F = 825$ cm	$U_r = 15$m/sec, $F = 345$cm

It is rather curious that the higher order approximation, Gram-Charlier (III), which has shown the best fit to the observed distribution of $\eta(t)$, is not good

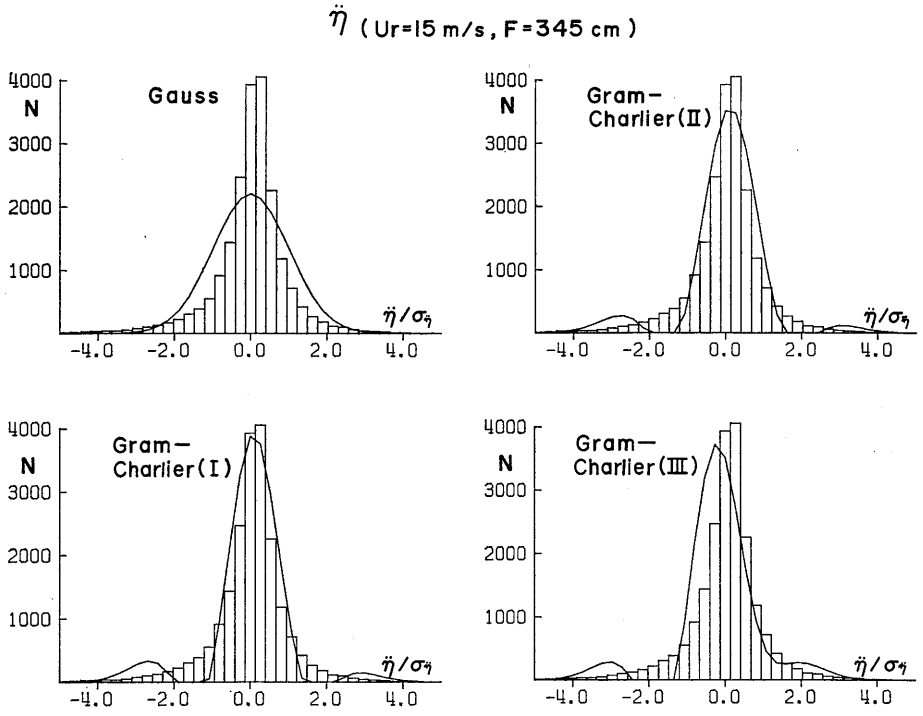

Fig. 3. The comparisons of the measured distributions for the vertical surface acceleration $\ddot{\eta}(t)$ with various theoretical distributions, Gaussian, Gram-Charlier (I), (II) and (III). Wave data ($F = 345$ cm, $U_r = 15$ m/sec).

for the distribution of $\ddot{\eta}(t)$ as compared the lower order approximation Gram-Charlier (I) and (II).

In Figures 4 and 5, typical examples of the measured distributions are compared with the Gaussian distributions (light curves) and the Gram-Charlier (III) distributions (heavy curves). The figures show the statistical distributions of $\eta(t)$ (upper curves), $\dot{\eta}(t)$ (middle curves) and $\ddot{\eta}(t)$ (lower curves) at $F = 105$ cm and 345 cm, for $U_r = 5$, 10, 15 m/sec. In Figure 6 are shown the statistical distributions of $\eta(t)$ at $F = 585$ cm and 825 cm for the above wind velocities. The values of various quantities relating to the measured distributions, *i.e.*, variance σ^2, skewness $\sqrt{\beta_1}$ ($\equiv\lambda_3$), kurtosis β_2 ($\equiv\lambda_4$) and sum of χ^2 are summarized in Tables 1, 2, and 3. These tables includes the data on the statistical distributions which are not shown in Figures 4, 5 and 6. In Figures 7 and 8 the skewness $\sqrt{\beta_1}$ and the kurtosis β_2 of the measured distributions for $\eta(t)$, $\dot{\eta}(t)$ and $\ddot{\eta}(t)$ are plotted against the reference wind speed U_r.

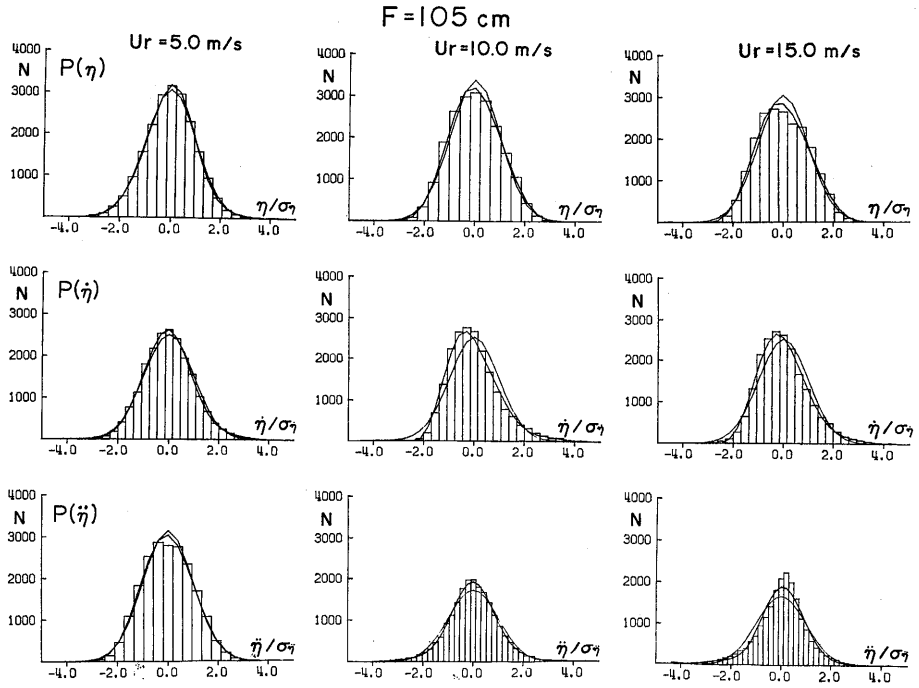

Fig. 4. The measured distributions of the wind-generated waves with theoretical distributions, Gaussian (light curve) and Gram-Charlier (III) (heavy curve). From top to bottom; surface elevation $\eta(t)$, vertical surface velocity $\dot{\eta}(t)$ and vertical surface acceleration $\ddot{\eta}(t)$. Wave data ($F = 105$ cm, $U_r = 5$, 10, 15 m/sec).

5. Discussions

5-1. The distribution of the surface elevation $\eta(t)$ and the vertical velocity $\dot{\eta}(t)$

The following characteristics of the distributions for $\eta(t)$ and $\dot{\eta}(t)$ can be seen from the results shown in Figures 4 through 8 and Tables 1, 2 and 3.

When wind waves are generated at very short fetches and low wind speeds, the distributions for $\eta(t)$ and $\dot{\eta}(t)$ are given fairly accurately by both the Gram-Charlier (III) and Gaussian. The empirical fit is a little better for the Gram-Charlier (III) than for the Gaussian, but there are no appreciable differences. This indicates that the nonlinear effects are very weak at the initial stage of the generation of wind waves. With increasing fetches and wind speeds, the deviations of the observed distribution from the Gaussian distribution increase gradually, and the distributions can be better expressed by the Gram-Charlier (III).

However, the range over which the Gram-Charlier (III) is effectively

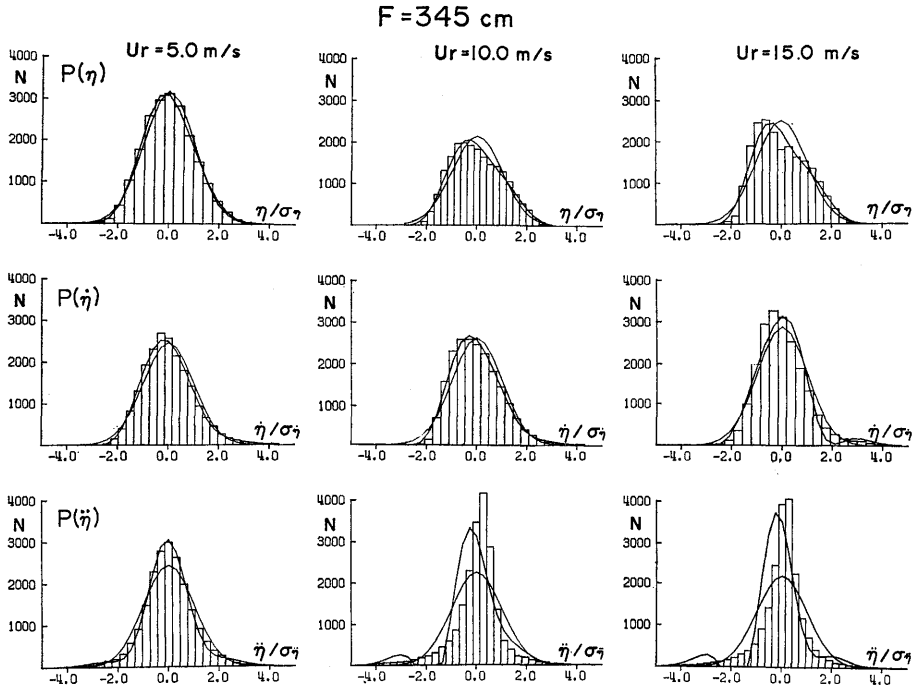

Fig. 5. The measured distributions of the wind-generated waves with theoretical distributions, Gaussian (light curve) and Gram-Charlier (III) (heavy curve). From top to bottom; surface elevation η (t), vertical surface velocity $\dot{\eta}(t)$ and vertical surface acceleration $\ddot{\eta}(t)$. Wave data ($F = 345$ cm, $U_r = 5$, 10, 15 m/sec).

applied is not so wide as would be expected. With increasing fetches and wind speeds the distributions deviate gradually from the Gram-Charlier (III). It should be mentioned here that the values of $\Sigma\chi^2$ for the Gram-Charlier (III) increase greatly at $U_r = 10$ m/sec except for the case of relatively long fetches (F: 585, 825 cm).

The distributions for $\dot{\eta}(t)$ show the similar characteristics as those for $\eta(t)$. The variances of the distributions for $\eta(t)$ and $\dot{\eta}(t)$ increase with increasing wind speeds and fetches. In our previous paper (MITSUYASU and HONDA[7),8)]) it has been shown that the increases of $\overline{\eta^2}$ follow to the universal fetch relations except for the data corresponding to very low wind speeds. With increasing wind velocity, the skewness $\sqrt{\beta_1}$ of the distributions for $\eta(t)$ and $\dot{\eta}(t)$, and the kurtosis β_2 for $\dot{\eta}(t)$, increase slowly, but the kurtosis β_2 of $\eta(t)$ decreases slightly. The skewness $\sqrt{\beta_1}$ and the kurtosis β_2 of the distributions for $\eta(t)$ and $\dot{\eta}(t)$ seem to depend not so much on fetch. As shown in Figures 7 and 8, both $\sqrt{\beta_1}$ and β_2 for $\dot{\eta}(t)$ are larger than those for $\eta(t)$. Approximate ranges for the values of $\sqrt{\beta_1}$ and β_2 are

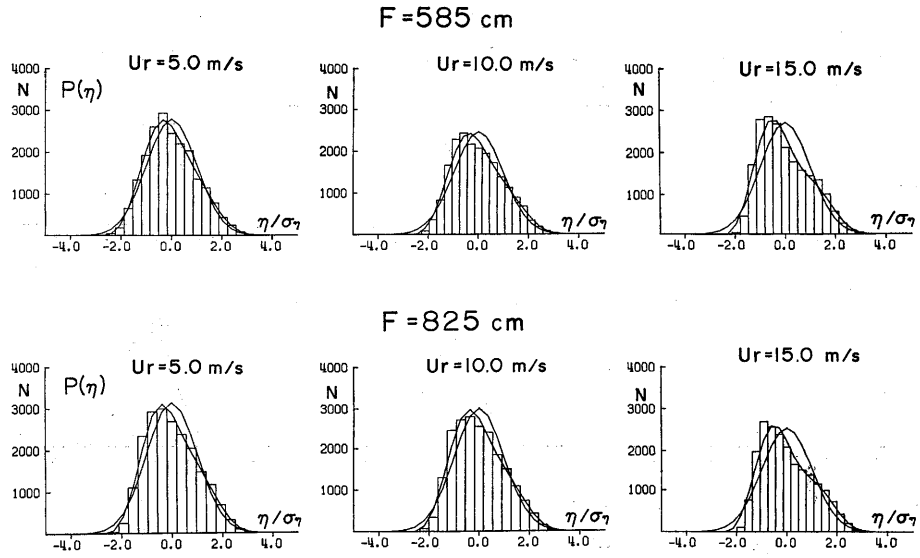

Fig. 6. The measured distributions for surface elavation $\eta(t)$ of the wind-generated waves with theoretical distributions, Gaussian (light curve) and Gram-Charlier (III) (heavy curve). Wave data ($F = 585$ cm (upper) and $F = 825$ cm (lower), $U_r = 5$, 10, 15 m/sec).

summarized as follows:

	$\sqrt{\beta_1}$	β_2
$\eta(t)$	$-0.1 \sim 0.5$	$2.4 \sim 3.3$
$\dot{\eta}(t)$	$0.3 \sim 0.9$	$3.2 \sim 5.1$

5-2. The distribution of the surface vertical acceleration $\ddot{\eta}(t)$

The distribution for $\ddot{\eta}(t)$ shows slightly different characteristics as compared with the distributions for $\eta(t)$ and $\dot{\eta}(t)$.

At the initial stage of the generation of wind waves, *i.e.*, for the cases of low wind speeds and short fetches, the skewness $\sqrt{\beta_1}$ of the distributions of $\ddot{\eta}(t)$ shows positive small values and the distributions can be well approximated by the Gram-Charlier (III). When wind speeds and fetches are increased, however, $\sqrt{\beta_1}$ changes at some wind speed from positive small values to relative large negative values as shown in Figure 11. The kurtosis β_2 for $\ddot{\eta}(t)$ increases sharply with increasing wind speeds.

The fact that the skewness of the distribution for $\ddot{\eta}(t)$ shows negative value in constrast to the positive skewnesses of those for $\eta(t)$ and $\dot{\eta}(t)$, can be well understood when we consider the following situations. With increasing wind speeds and fetches, nonlinear characteristics of wind waves increase gradually and wave forms show the asymmetical form with respect both to

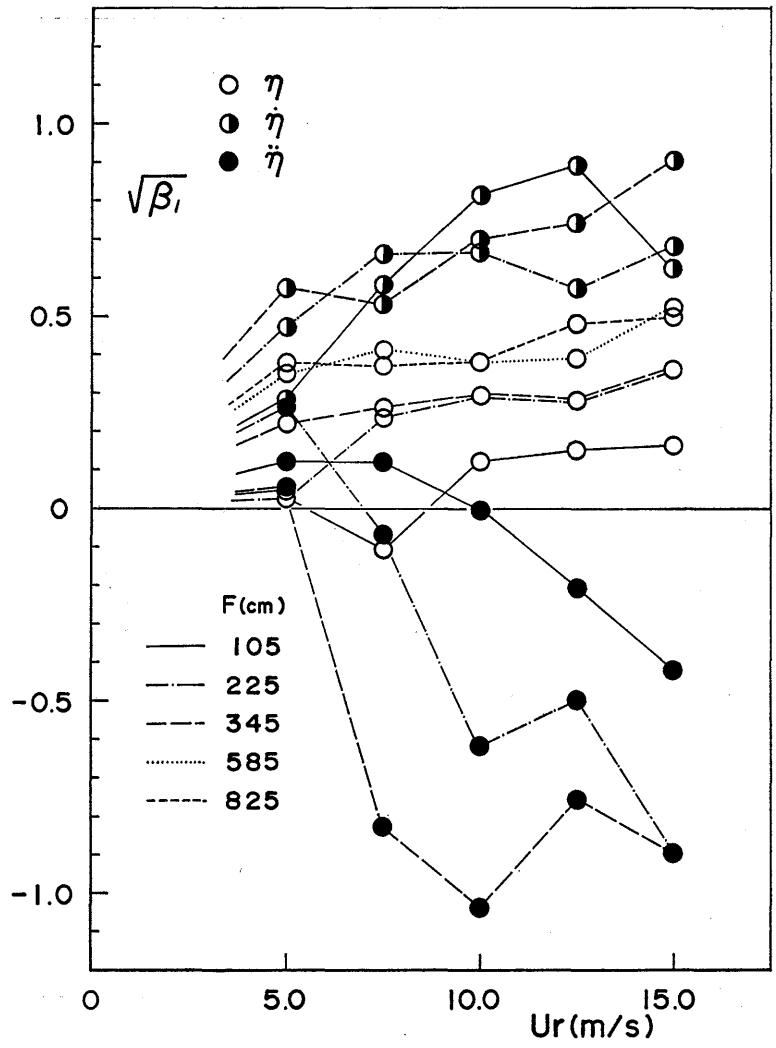

Fig. 7. The skewness of the distributions for surface elevation $\eta(t)$, vertical surface velocity $\dot{\eta}(t)$ and vertical surface acceleration $\ddot{\eta}(t)$ of the wind-generated waves.

still water level and to wave crest. That is, the wave crest becomes sharper and narrower and the wave trough becomes flatter and wider. Moreover, wave breaking is caused at the crest of the wind wave. Such characteristics of the wave forms make the distributions of $\eta(t)$ concentrate to relatively narrow range for negative side and widely scatter to the positive side. Therefore, the skewness of the distribution for $\eta(t)$ shows positive values. The positive skewness of the distributions for $\dot{\eta}(t)$ correspond both to the

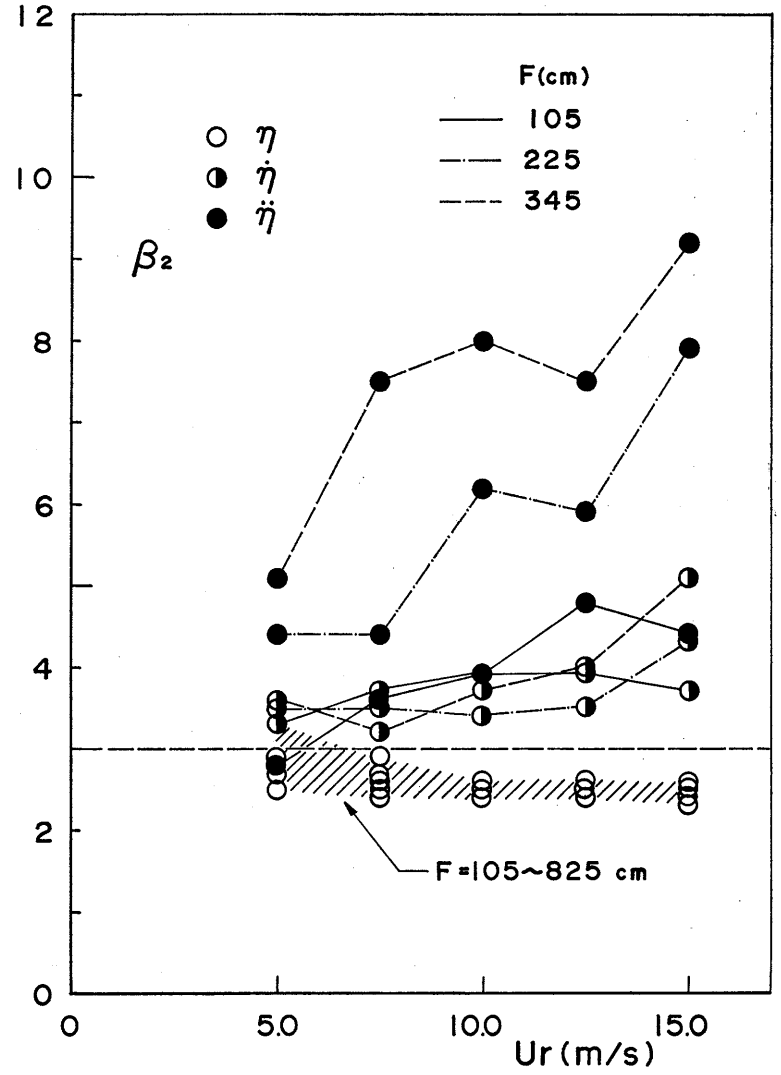

Fig. 8. The kurtosis of the distributions for surface elevation $\eta(t)$, vertical surface velocity $\dot{\eta}(t)$ and the vertical surface acceleration $\ddot{\eta}(t)$ of the wind-generated waves.

forward inclinations of the wave form and to the irregularity of the front face of wave crest. The former is caused mainly by the wind stress and the latter is caused by the wave breaking. The vertical surface acceleration $\ddot{\eta}(t)$ have negative values at the wave crest and positive values at the wave trough. That is, the sign for $\ddot{\eta}(t)$ is reverse of that for $\eta(t)$. This is the reason why the skewness of the distribution for $\ddot{\eta}(t)$ shows negative values

Table 1. The statistical properties of the distributions for surface elevation $\eta(t)$ of the wind-generated waves (degree of freedom=21).

F m	Ur m/s	$\bar{H}$ cm	$\bar{T}$ sec	σ_η cm	$\sqrt{\beta_1}$	β_2	Gram-Charlier (III) $\Sigma\chi^2$	Gauss $\Sigma\chi^2$
1.05	5	0.02	0.06	1.06×10^{-2}	0.042	3.31	4	13
	7.5	0.10	0.07	4.67×10^{-2}	-0.111	2.92	9	27
	10	0.22	0.10	9.65×10^{-2}	0.116	2.58	39	203
	12.5	0.38	0.13	1.57×10^{-1}	0.148	2.44	81	345
	15	0.64	0.15	2.69×10^{-1}	0.165	2.50	94	360
2.25	5	0.07	0.08	3.11×10^{-2}	0.032	2.89	7	7
	7.5	0.20	0.11	9.08×10^{-2}	0.227	2.73	11	196
	10	0.59	0.17	2.39×10^{-1}	0.294	2.44	76	599
	12.5	0.75	0.19	3.12×10^{-1}	0.281	2.53	22	350
	15	1.45	0.23	5.77×10^{-1}	0.364	2.58	69	707
3.45	5	0.12	0.11	5.14×10^{-2}	0.225	2.86	10	89
	7.5	0.46	0.18	1.83×10^{-1}	0.257	2.59	27	301
	10	0.95	0.23	3.81×10^{-1}	0.285	2.36	108	701
	12.5	1.18	0.25	4.64×10^{-1}	0.286	2.39	146	796
	15	2.18	0.31	8.18×10^{-1}	0.362	2.31	279	1344
5.85	5	0.30	0.12	1.46×10^{-1}	0.346	2.71	55	386
	7.5	0.93	0.22	3.87×10^{-1}	0.411	2.53	85	835
	10	1.43	0.27	5.93×10^{-1}	0.378	2.54	105	767
	12.5	1.70	0.27	7.28×10^{-1}	0.390	2.61	63	596
	15	3.03	0.34	1.22×10^{-1}	0.524	2.50	216	1850
8.25	5	0.62	0.19	2.60×10^{-1}	0.384	2.55	79	764
	7.5	1.54	0.29	5.93×10^{-1}	0.370	2.36	156	1034
	10	2.08	0.33	8.20×10^{-1}	0.383	2.54	99	754
	12.5	2.69	0.35	1.08×10^{0}	0.478	2.62	68	970
	15	3.94	0.39	1.63×10^{0}	0.496	2.39	195	1781

$\bar{H}$: The mean values of wave heights defined by the zero-up-crossing method
$\bar{T}$: The mean values of wave periods defined by the zero-up-crossing method

in contrast to the positive skewness of those for $\eta(t)$. The above discussion may cause some misunderstanding that the wave form of the random sea surface is confused with that of the nonlinear wave of a single period. However, the individual forms of dominant waves in a realized random sea surface are very close to those of slightly deformed nonlinear waves with corresponding periods (see for example, CHANG *et al*[9]).

In a range of relatively low wind speeds the variance of the distribution for $\dot{\eta}(t)$ is approximately proportional to the wind speed but increasing rate

Table 2. The statistical properties of the distributions for vertical surface velocity $\dot{\eta}(t)$ of the wind-generated waves (degree of freedom=27).

F m	Ur m/s	$\sigma_{\dot{\eta}}/2\pi$(cm/sec)	$\sqrt{\beta_1}$	β_2	Gram-Charlier (III) $\Sigma\chi^2$	Gauss $\Sigma\chi^2$
1.05	5	9.24×10^{-2}	0.279	3.48	14	67
	7.5	6.10×10^{-1}	0.575	3.70	33	316
	10	9.13×10^{-1}	0.809	3.89	51	682
	12.5	1.24×10^{0}	0.890	3.93	62	1065
	15	1.85×10^{0}	0.617	3.75	38	458
2.25	5	3.85×10^{-1}	0.466	3.64	47	202
	7.5	7.43×10^{-1}	0.655	3.55	12	470
	10	1.35×10^{0}	0.660	3.44	41	543
	12.5	1.68×10^{0}	0.575	3.52	7	349
	15	2.70×10^{0}	0.677	4.27	70	343
3.45	5	4.67×10^{-1}	0.567	3.65	24	230
	7.5	1.03×10^{0}	0.532	3.19	20	374
	10	1.72×10^{0}	0.703	3.66	58	627
	12.5	1.98×10^{0}	0.745	4.03	101	558
	15	3.13×10^{0}	0.904	5.08	359	536

Table 3. The statistical properties of the distributions for vertical surface acceleration $\ddot{\eta}(t)$ of the wind-generated waves (degree of freedom=41 (*=21)).

F m	Ur m/s	$\sigma_{\ddot{\eta}}/(2\pi)^2$(cm/sec^2)	$\sqrt{\beta_1}$	β_2	Gram-Charlier (III) $\Sigma\chi^2$	Gauss $\Sigma\chi^2$
1.05	5	2.37×10^{0}	0.118	2.77	51*	131*
	7.5	1.75×10^{1}	0.118	3.65	22	108
	10	2.12×10^{1}	−0.007	3.94	12	124
	12.5	2.43×10^{1}	−0.214	4.78	888	1595
	15	3.37×10^{1}	−0.424	4.42	216	589
2.25	5	9.70×10^{0}	0.264	4.35	51	195
	7.5	1.51×10^{1}	−0.073	4.36	83	350
	10	1.74×10^{1}	−0.620	6.21	703	1880
	12.5	2.27×10^{1}	−0.502	5.92	721	1646
	15	4.35×10^{1}	−0.898	7.94	2054	2127
3.45	5	1.03×10^{1}	0.050	5.05	23	334
	7.5	1.31×10^{1}	−0.834	7.48	1314	2188
	10	1.79×10^{1}	−1.044	7.97	2087	3079
	12.5	2.30×10^{1}	−0.758	7.48	1360	2266
	15	4.57×10^{1}	−0.899	9.17	2260	3443

becomes gradually smaller and shows a tendency to saturate for high speed wind. The kurtosis β_2 of the distribution for $\ddot{\eta}(t)$ is exceedingly larger than that of the Gaussian. The skewness $\sqrt{\beta_1}$ seem to depend not so much on fetch, but the kurtosis β_2 increases remarkably with increasing fetch.

6. Concluding remarks

General conclusions of the present study are as follows. For the wind waves generated at short fetches and low wind speeds, in other words, for the wind waves with weak nonlinearity, the higher order approximation of the nonlinear theory of LONGUET-HIGGINS[6] can be effectively applied for the statistical distribution of the wind-wave surface.

The following question will be naturally arisen: Whether or not the higher the order of approximation is the better the agreement between the theoretical distribution and the observed one? To answer this question we have tried to compare the measured distributions with theoretical ones in which the order of approximation is higher than in (11). However, the agreements between the theory and experiment have not been improved. The results are considered to be due to the following reasons. The higher order approximation includes the higher order moments of the distribution. But the accuracy of the measured higher order moments are not so good. Furthermore, the measured distributions of the elevation of the wind waves with fairly strong nonlinearity are affected by the wave breaking, particularly when the wind speed is relatively high. The effects of wave breaking on the statistical distribution of wave surface can not be treated by such a theory as presented by LONGUET-HIGGINS[6].

Acknowledgements

Much of this work was assisted by Mr. K. ETO, to whom the authors owe thanks for his co-operation in carrying out the experiment and for preparing figures. The authors also express their gratitudes to Mr. M. TANAKA for his assistance in the numerical computation and to Miss N. URAGUCHI for the typing of the manuscript. A part of this work was supported by scientific research fund from the Ministry of Education.

References

1) RUDNICK, P.: Correlograms for Pacific ocean waves. Proc. 2nd Berkeley Symposium on Mathematical Statistics and Probability. Berkeley, University of California Press, 1950, pp. 627-638.
2) PIERSON, W. J.: Wind-generated gravity waves. Advances in Geophysics, 2. New York, Academic Press, Inc., 1955, pp. 93-178.
3) LONGUET-HIGGINS, M. S., D. E. CARTWRIGHT and N. D. SMITH: Observations of

the directional spectrum of sea waves using the motions of a floating buoy. Ocean Wave Spectra. Englewood Cliffs, N. J., Prentice-Hall, Inc., 1961, pp. 111-132.
4) KINSMAN, B.: Surface waves at short fetches and low wind speed—a field study. Chesapeake Bay. Inst., Tech. Rep., No. 19, 1960.
5) MITSUYASU, H. : Wind wave in decay area. Report of Port & Harbour Technical Research Inst., No. 5, 1964.
6) LONGUET-HIGGINS, M. S.: The effect of nonlinearities on statistical distributions in the theory of sea waves. J. Fluid Mech., 17, 1963, pp. 459-480.
7) MITSUYASU, H. and T. HONDA: The high frequency spectrum of wind-generated waves. J. Oceanog. Soc. Japan, 30, 1974, pp. 185-198.
8) MITSUYASU, H. and T. HONDA: The high frequency spectrum of wind-generated waves. Rep. Res. Inst. Appl. Mech. Kyushu Univ. Vol. 22, No. 71, 1975, pp. 327-355.
9) CHANG, P. C., E. J. PLATE and G. M. HIDY: Turbulent air flow over the dominant component of wind-generated water waves. J. Fluid Mech., 47, 1971, pp. 183-208.

(Received April 28, 1976).